Neural expressiveness for beyond importance model compression

Anonymous Author(s)
Affiliation
Address
email

Abstract

Neural Network Pruning has been established as driving force in the exploration of memory and energy efficient solutions with high throughput both during training and at test time. In this paper, we introduce a novel criterion for model compression, named “Expressiveness". Unlike existing pruning methods that rely on the inherent “Importance" of neurons’ and filters’ weights, “Expressiveness" emphasizes a neuron’s or group of neurons ability to redistribute informational resources effectively, based on the overlap of activations. This characteristic is strongly correlated to a network’s initialization state, establishing criterion autonomy from the learning state (*stateless*) and thus setting a new fundamental basis for the expansion of compression strategies in regards to the “When to Prune" question. We show that expressiveness is effectively approximated with arbitrary data or limited dataset’s representative samples, making ground for the exploration of *Data-Agnostic strategies*. Our work also facilitates a “hybrid" formulation of expressiveness and importance-based pruning strategies, illustrating their complementary benefits and delivering up to 10× extra gains w.r.t. weight-based approaches in parameter compression ratios, with an average of 1% in performance degradation. We also show that employing expressiveness (independently) for pruning leads to an improvement over top-performing and foundational methods in terms of compression efficiency. Finally, on YOLOv8, we achieve a 46.1% MACs reduction by removing 55.4% of the parameters, with an increase of 3% in the mean Absolute Precision (mAP_{50-95}) for object detection on COCO dataset.

1 Introduction

To address the computational constraints of existing models, Model Compression [7] has emerged as a prominent solution in exploring models that achieve comparable performance, but with reduced computational complexity [52]. Within this scope, Floating Point Operations (*FLOPs*) are used to estimate a model’s computational complexity, by measuring the arithmetic operations required for a forward pass, while parameters (*params*) are associated with a model’s size in terms of memory space [48] and their reduction can be a precursor towards more energy efficient solutions [5]. Although *FLOPs* and *params* often correlate, their relationship isn’t strictly linear. For instance, VGG16 [43] has 17× more parameters than ResNet-56 [17] but only 3× more *FLOPs*, largely due to VGG16’s extensive use of fully connected layers. At first sight, this can be attributed to the differences in network topologies. From a deeper perspective, the intricacies of various operations at handling computational workloads, such as residual structures [17, 55], depthwise separable convolutions [19], inverted residual modules [18], channel shuffle operations [59] and shift operations [53], coupled with their interplay, may significantly affect the relationship between *FLOPs* and *params* in a neural network. In a nutshell, besides the use of more computationally efficient operations as above-mentioned, Model Compression aims to maintain model performance while optimizing the two aforementioned metrics via tensor decomposition, data quantization, and network sparsification [7].

In this paper we emphasize on the sparsification strategy of pruning [49], which we use as a basis framework to introduce **“Expressiveness"** as a new criterion for compressing neural networks. Existing pruning methods focus on removing redundant network elements – be they weights, neurons, or structures of neurons – in ways that minimally affect the overall performance of a network, based on the criterion of **“Importance"**, e.g. [38, 58, 20, 30]. Importance-based methods address questions like “How much does the removal of a network's element cost in terms of performance degradation?" and “How much information does a network element contain?" in various ways. More specifically, they are motivated by the information inherent in network elements, such as the magnitude of weights [15, 28], similarity of weights or weight matrices [29, 60] ; and their sensitivity to the network's loss function, such as the magnitude of gradients [38] and more [49, 3]. Such dependencies on weights' distributions constitute the aforementioned pruning methods to be “data-aware" since they intrinsically rely on the input data and the information state of the model, making the importance estimation of the network's elements challenging and often costly due to factors like i) the stochasticity from training with minibatches, ii) the presence of plateau areas in the optimization space, and iii) the complexity introduced by nonlinearities [38]. Liu et al. [36] have also discussed limitations in the perception of importance within trained models, i.e. the authors criticize the ability of network's elements importance to generalize to pruned derivatives, while also questioning the necessity of training large-scale models prior pruning.

Inspired by the concepts of “Information Plasticity" [2] and the “Lottery Ticket Hypothesis" (LTH) [12], we aim to address the limitations of previous importance-based methods through elaborating the “Expressiveness" criterion in model compression. In contrast to “Importance", we focus on understanding the capability of network elements to redistribute informational resources to subsequent network elements. We define “Expressiveness" as - “*A neuron's or group's of neurons potential (when a network is not fully trained) or ability (when it is trained) to extract features that maximally separate different samples*". As derived by [2], the early training phase of a model is crucial in shaping its expressiveness, with the formation of critical paths —strong connections that determine the “workload distribution"— being particularly significant during these initial stages. It's essential to note that the network's initialization state influences the formation of those paths, which interestingly enables "Expressiveness" to be a fit criterion for compression during all time instances of a networks' convergence [12], setting a baseline for answering the question of "When to prune?" [42]. *Our proposed pruning metric centers on measuring the overlap of activations between datapoints of the feature space*. In that way, expressiveness is based on effectively evaluating the inherent ability of the network's neurons to differentiate sub-spaces within the feature space. We experimentally show that utilizing either small sets of arbitrary data points from the feature space or stratified sampling [34] from each class yields consistent estimations of expressiveness. Finally, we propose and implement a new “hybrid" pruning optimization strategy that cooperatively searches, exploits and characterizes the complementary benefits between “Importance" and “Expressiveness" for model compression. In summary, this work offers the following four-fold contribution: (i) we propose Expressiveness, a novel criterion based on the overlap of activations for model compression; (ii) we provide an in-depth theoretical analysis of both the fundamental principles and the technical intricacies of the proposed criterion; (iii) we validate the hypothesis that Expressiveness can be approximated with little to none input data, opening the road for data-agnostic pruning strategies; and (iv) through extensive experimentation we offer a thorough comparison w.r.t to both foundational and state-of-the-art methods demonstrating the efficiency and effectiveness of the proposed technique in model compression, while also examining the feasibility and effectiveness of a “hybrid" expressiveness-importance pruning strategy.

Specifically, we validate “Expressiveness" on the CIFAR-10 [24] and ImageNet [40] datasets using a variety of models with different design characteristics [44, 17, 45, 21, 19]. We demonstrate the superiority of our novel criterion over existing solutions, including many top performing structural pruning methods [31, 61, 58, 32, 23, 46, 11], and show significant params reduction while maintaining comparable performance. We experimentally explore and analyze the complementary nature of expressiveness and importance, showing that summary numeric evaluation provides up to 10× additional parameter compression ratio gains, with an average of 1% loss decrease w.r.t group ℓ1-norm [28]. Finally, we experiment on the current state-of-the-art computer vision model (YOLOv8 [9, 22]), showcasing notable compression rates of 53.9% together with performance gains of 3% on the COCO dataset [33], and highlighting the ability of more expressive neurons to better recover lost information from the pruning operation.

2 Related Work

Weight (Non-Structural) Importance. Han et al. [15, 14] and Guo et al. [13] approached the importance of weights based on their magnitude, removing connections below given thresholds. However, earlier works [25, 16] emphasized on the Hessian of the loss and have questioned whether magnitude is a reliable indicator of weight's importance, as small weights can be necessary for low error. In this direction, several studies [4, 47, 41, 8] have proposed strategies of iterative magnitude pruning, in the form of "adaptive weight importance", where weights are ranked based on their sensitivity to the loss. From a different perspective, Yang et al. [56] address the limitations of individual weight's saliency that fail to account for their collective influence and provide a formulation of weight's importance based on the error minimization of the output feature maps. Expanding on this concept, Xu et al. [54] propose a layer-adaptive pruning scheme that encapsulates the intra-relation of weights between layers, focusing on minimizing the output distortion of the network. Amongst other factors and limitations (as also discussed in 1), weight importance is very expensive to measure, mainly because of the increased complexity induced by the mutual influences of the weights among interconnected neurons. This, coupled with the requirement for specialized hardware to manage the irregular sparsity patterns resulting from weight pruning [57], has shifted research focus towards structural pruning [28], where neurons or entire filters are removed.

Neuron and Filter (Structural) Importance. Many where driven by the success of Iterative Shrinkage and Thresholding Algorithms (ISTA) [6] in non-structural sparse pruning and proposed filter-level adaptations [28, 29, 32, 26], based on the relaxation ($\ell 1$ and $\ell 2$) of $\ell 0$ norm minimization. However, the loss of universality of such magnitude-based methods remains a limitation in the approximation of importance even in the structural scope. Yu et al. [58] further elaborate on the idea of error propagation ignorance, where the analysis is limited to the statistical properties of a single [28, 29] or two consecutive layers [37]. The authors suggest that the importance of neurons is better approximated from the minimization of the reconstruction error in the final response layer from which it is propagated to previous layers. In contrast to this view, Zhuang et al. [61] emphasize on the discriminative power of a filter as a more effective measure of importance and highlight that this aspect is not effectively assessed by the minimization of the reconstruction error. In a manner that reflects the progression of weight importance, Molchanov et al. [38] define "adaptive filter importance" as the squared change in loss and apply first and second-order Taylor expansions to accelerate importance's computations. Predominantly, the data-awareness imposed by most pruning strategies is added to their already high-complexity – i.e. mostly non-convex, NP-Hard problems that require combinatorial searches. This renders the estimation of importance both computationally expensive and labor-intensive, similarly to non-structural approaches. Notably, Lin et al. [30] propose a less data-dependent solution based on the observation that the average rank of multiple feature maps generated by a single filter remains constant. HRank [30], alongside several other feature-guided filter pruning approaches, are valuable indicators towards data independence. Such works form a principle that pruning elements are better evaluated in the activation phase, where the importance of information and the richness of characteristics for both input data and filters are better reflected. In this work, we expand on this belief and we through extensive experimental analysis, we demonstrate that neither the information state nor the input data is required for the discriminative characterization of an element.

3 Neural Expressiveness

3.1 Weights and Activations: Importance vs Expressiveness

Neurons are the main constituent element of a neural network. Given a neural network $\mathcal{N}$, we denote neurons by $a_i^{(l)}$, where $l \in L$ is indicative of the neuron's layer in a network with $L = \{l_0, ..., l_l, ..., l_{|L|}\}$ layers and i of its position in the given layer $l = \{a_0, ..., a_i, ..., a_{|l|}\}$. Another important element are the learning parameters of the network. Otherwise the weights represent the strength of connections between neurons in adjacent layers and are denoted by $w_{ij}^{(l)}$, where i and j index the neurons in the current and previous layers. In that manner, neuron's can be perceived as switches that allow or block information from propagating through-out a network. The activation (or not) of a neuron $a_i^{(l)}$ depends on the output value of its activation function $\sigma(\cdot)$, where there are many popular options for the definition of σ, e.g., sigmoid, tanh, and ReLU functions. Specifically, a neuron's output is defined as follows,

$$a_i^{(l)} = \sigma\left(\sum_j w_{ij}^{(l)} a_j^{(l-1)} + b_i^{(l)}\right) \tag{1}$$

where $b_i^{(l)}$ denotes the bias term. From eq. 1, we observe that a neuron's activation is affected by the activation of the previous layers, hence affecting in the same way the consecutive layers. This interdependence between activations $a^{(l)}$, for a given layer l defines a recurrent form that can be generalized as follows,

$$a^{(l)} = \sigma\left(W^{(l)} f\left(a^{(l-2)}, \ldots, a^{(1)}\right) + b^{(l)}\right). \tag{2}$$

On the other hand, weights are a more static representation of information as they modulate how much influence one neuron's activation has on another's, compared to activations that control the flow of information in a network. This differentiation has motivated us to define two axes of study in the categorisation of pruning criteria, one based on the weights ("importance") and one based on the activation phase ("expressiveness").

Generalization of concepts in a structural level. The aforementioned principles extend to the structural representations of weights and activations, the most common being Convolutional Neural Networks (CNNs). For a CNN model with a set of K convolutional layers, where C^l is the $l-th$ convolutional layer. We denote filters (weight maps) and feature maps (activation maps) as F_k^l and C_k^l respectively, where k the is index within a layer. Given filter with dimensions $m \times n$, eq. 1 is adapted as follows,

$$C_k^{(l)}(x,y) = \sigma\left(\sum_{i=1}^{m}\sum_{j=1}^{n} F_{ij}^{(l,k)} a_{x+i-1,y+j-1}^{(l-1)} + b_k^{(l)}\right) \tag{3}$$

where (i,j) and (x,y) are the coordinates of weights and output activations within the filter and the output activation map respectively. Similarly, a convolution layer l can be analyticaly expressed as follows,

$$C^{(l)} = \begin{cases} \sigma\left(\bigoplus_{k=1}^{K^{(1)}} F^{(1,k)} * X + B^{(1)}\right) & \text{if } l = 1 \\ \sigma\left(\bigoplus_{k=1}^{K^{(l)}} F^{(l,k)} * C^{(l-1)} + B^{(l)}\right) & \text{if } l > 1 \end{cases} \tag{4}$$

with X being the input to the first layer of the network, and where symbol $*$ denotes convolution operation and $\bigoplus$ denotes the concatenation operation. Within this context[1], eq. 2 is generalized as follows,

$$C^{(l)} = \sigma\left(\bigoplus_{k=1}^{K^{(l)}} F^{(l,k)} * f\left(C^{(l-2)}, \ldots, C^{(1)}\right) + B^{(l)}\right). \tag{5}$$

Conceptualization of information propagation. Consider a task with $X = \{x_i\}_{i=1}^{|D|}$ denoting dataset samples, where $|D|$ is the size of the dataset. Given the information state (weight state) of a CNN model with K convolutional layers at a given time t_i, X is mapped through the network as $f(X, W_{t_i})$, where $W_{t_i} = \{F_{t_i}^1, \ldots, F_{t_i}^l, \ldots, F_{t_i}^{|K|}\}$ and $F_{t_i}^l = \{F_{t_i}^{(l,1)}, \ldots, F_{t_i}^{(l,k)}, \ldots, F_{t_i}^{(l,K^{(l)})}\}$, with $K^{(l)}$ being the amount of weight maps (filters) in a given layer l. This process can be further analyzed as follows,

$$f(X, \mathbf{W}_{t_i}) = \mathcal{F}_{|K|}(\mathcal{F}_{|K|-1}(\ldots \mathcal{F}_1(X; \mathbf{F}_{t_i}^1); \mathbf{F}_{t_i}^2); \ldots; \mathbf{F}_{t_i}^{|K|}), \tag{6}$$

where $\mathcal{F}_l$ represents the mapping operation of convolutional layer l.

Based on eq. 2 and eq. 5, the equivalent of the previous based on the activations of the layers can be expressed as,

$$f(X, \mathbf{W}_{t_i}) = C^{(|K|)}\left(\ldots\left(C^{(2)}\left(C^{(1)}\left(X, \mathbf{F}_{t_i}^1\right), \mathbf{F}_{t_i}^2\right) \ldots\right), \mathbf{F}_{t_i}^{|K|}\right). \tag{7}$$

[1]We do not include pooling and batch normalization layers in the formulations; however, the equations can be expanded to incorporate them as intermediate steps based on each architecture.

Here, $C^{(l)}$ represents the activation map of the l-th layer, where $C^{(l)} = \mathcal{F}_l(C^{(l-1)}; \mathbf{F}^l_{t_i})$ aligns with the structure defined in eq. 4. In this formulation, $C^{(1)}$ is the activation map of the first layer, computed using the input X and the first layer's filters $\mathbf{F}^1_{t_i}$. Subsequent layers' activation maps $C^{(l)}$ are derived from the previous layer's output $C^{(l-1)}$ and their respective filters $\mathbf{F}^l_{t_i}$. Assuming a classification task, the final layer $C^{(|K|)}$ is considered the classification layer, effectively summarizing the hierarchical feature extraction and transformation process across all convolutional layers.

3.2 Mathematical Foundation of Neural Expressiveness.

We observe that the training parameters of the model, in this case ${W_{t_i}}$[2], are responsible for transforming the original input feature space X into a sequence of intermediate feature spaces$\{C^{(1)}, \ldots, C^{(|K|-1)}\}$, progressing towards the final prediction formulated by the prediction layer $C^{(|K|)}$.

Based on this intrinsic characteristic of neural networks and inspired by the goal of optimizing feature discrimination, akin to the entropy reduction strategy in decision trees [51], we assess network elements ability, in this scenario filters, to extract features, i.e., activation patterns, that maximally separate different input samples x_i. In other words, we score the expressiveness of the filters within W_{t_i}, based on the discriminative quality of the intermediate feature spaces they generate, where the feature space generated by a filter F^l_k, is denoted as C^l_k.

Neural Expressiveness foundational concept. When assessing the expressiveness of an element within W_{t_i} based on its generated feature spaces, e.g., $NEXP(F^l_{t_i}; C^l)$, we cooperatively evaluate all of its preceding elements, as derived from eq. 5. This can be formulated as,

$$NEXP(F^l_{t_i}; C^l) = NEXP(F^l_{t_i}; (C^{(l-1)}, C^{(l-2)}, \ldots, C^{(1)})), \tag{8}$$

which can be further extended to incorporate the inter-dependencies between the examined element and its predecessors, in accordance with eq. 7, as detailed below:

$$\begin{aligned} &NEXP\left(F^l_{t_i}; \left(C^{(l-1)}, C^{(l-2)}, \ldots, C^{(1)}\right)\right) = \\ &NEXP\left(F^l_{t_i}; \left((C^{(l-2)}, \mathbf{F}^{l-1}_{t_i}), (C^{(l-3)}, \mathbf{F}^{l-2}_{t_i}), \ldots, (X, \mathbf{F}^1_{t_i})\right)\right). \end{aligned} \tag{9}$$

The aforementioned eqs. 8 and 9 provide the *foundational concepts for utilizing the evaluation of the activation phase*, in an endeavor to encourage the development of more universal solutions by addressing the limitations of universality inherent in the assessment of the weight state alone (as also discussed in sections 1 and 2).

Formulation of Neural Expressiveness (NEXP) Score. Diving deeper into the Neural Expressiveness (NEXP) scoring process, we follow eq. 9 previously and assume a mini-batch $X^{'} = \{x^{'}_i\}_{i=1}^N$, with N being the number of samples in it. Mapping the batch through the network, based on eqs. 6 and 7, generates a set of sequences of feature spaces (activation maps), denoted as $S = \{s_1, \ldots, s_i, \ldots, s_N\}$, where $s_i = \{x^{'}_i, \ldots, C^l_i, \ldots, C^{|K|}_i\}$ is the sequence of the activation patterns generated from sample $x^{'}_i \in X^{'}$ and $|s_i| = |K| + 1$ is its cardinality, including the feature space of sample $x^{'}_i$. To evaluate a specific filter k in layer l, denoted as F^l_k, we utilize the retrieved activation patterns from that filter, denoted as $\{s^l_{i,k}\}_{i=1}^N$, where $s^l_{i,k} = C^l_{i,k}$ is the activation pattern retrieved from filter k in layer l.

To score the Neural Expressiveness of F^l_k, we first construct a $N \times N$ matrix that expresses all possible combinations of the activation patterns derived from the different input samples. This table can be visualised as follows,

$$\begin{pmatrix} s^l_{(1,1),k} & s^l_{(1,2),k} & \cdots & s^l_{(1,N),k} \\ s^l_{(2,1),k} & s^l_{(2,2),k} & \cdots & s^l_{(2,N),k} \\ \vdots & \vdots & \ddots & \vdots \\ s^l_{(N,1),k} & s^l_{(N,2),k} & \cdots & s^l_{(N,N),k} \end{pmatrix}. \tag{10}$$

[2]Bias terms are excluded for simplicity.

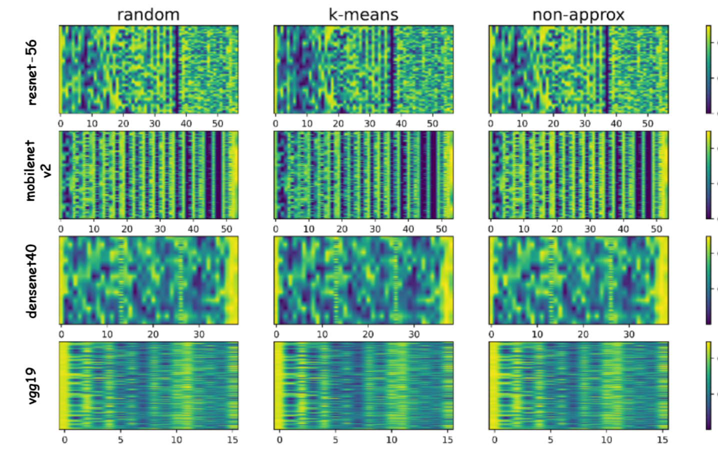

Figure 1: **Expressiveness statistics of feature maps from different convolutional layers and architectures on CIFAR-10.**

where $s^l_{(i,j),k}$ denotes the dissimilarity of activations patterns between the i-th and the j-th sample of the batch. In other words, the matrix in eq. 10 represents all the possible combinations of NEXP calculations, where each element $s^l_{(i,j),k}$ derives from $f(s^l_{i,k}, s^l_{j,k})$, with f being any dissimilarity function. Without loss of generality, for the rest of the study, we use the Hamming distance as the operator implementing dissimilarity function. Activations are first binarized (values greater than 0 become 1, and the rest become 0), i.e. enabling to evaluate the degree of overlap between the binary activation patterns using f.

We note that the matrix's diagonal, where i equals j, along with the elements below the diagonal, where i is greater than j, do not contribute additional value to quantifying the discriminative ability of an element. The diagonal elements represent comparisons of the same sample's activation patterns, rendering them redundant. Meanwhile, the lower triangular elements are considered duplicates since $s^l_{(i,j),k}$ is equal to $s^l_{(j,i),k}$, thereby not adding any new information. Drawing from these two observations, we define the Neural Expressiveness score (NEXP) as follows,

$$NEXP(F^l_k) = \frac{1}{\frac{N(N-1)}{2}} \sum_{i=1}^{N} \sum_{j=i+1}^{N} f(s^l_{i,k}, s^l_{j,k}) \tag{11}$$

The **more similar** the activation patterns derived from an element are, the **less expressive** it is declared to be. In eq. 11, we also normalize the score w.r.t the total amount of combinations ($\frac{N(N-1)}{2}$), thereby deriving the average expressiveness score. This average score is then utilized to characterize the discriminative capability/capacity of the examined network element. In this study, we used the mean operation, however, we note that alternate statistical measures, e.g., minimum, maximum, median, etc., could feasibly be applied in the computation of the overall score.

3.3 Dependency to Input Data

NEXP evaluates the inherent property of network elements to maximally distinguish between input samples. We extend this line of thought and assess its sensitivity to input data X and mini-batch size N, in order to delineate the dependence between NEXP and the input data. To achieve that, we perform a sensitivity analysis of NEXP to the mini-batch data X, using two input sampling strategies to assemble a batch with 60 samples, namely random sampling (denoted as 'random') and class-representative sampling via k-means (denoted as 'k-means'). We define the true NEXP score (denoted as 'non-approx') for each filter as the value obtained by comparing all activation patterns across the *entire training dataset* (more info in A.1). Fig. 1 presents a detailed comparative illustration of the results that highlight the similarities in NEXP estimations across various trained networks, including VGGNet [44], ResNet [17], MobileNet [19] and DenseNet [21] on CIFAR-10 dataset. Columns represent the aforementioned sampling strategies, while colors indicate expressiveness levels, with higher values signifying greater expressiveness. In each sub-figure, the x-axis indicates

Algorithm 1 NEXP Pruning Algorithm

Define: $NEXP_{\text{map}} = \{\{NEXP(F_k^l)\}_{k=1}^{|C^l|}\}_{l=1}^{|K|}$
Require: A mini-batch X, a neural network $\mathcal{N}(W_{t_i})$, a theoretical speed-up target, denoted τ, and the allowed amount of pruning steps, denoted $\text{steps}_{\text{max}}$.
Ensure: $\frac{\text{FLOPs}(\mathcal{N})}{\text{FLOPs}(\mathcal{N}_{\text{pruned}})} \geq \tau$

```
Initialize NEXP_map ← f(X; W_{t_i})
Initialize τ_current as 1
Initialize steps_current as 1
Initialize N_pruned as N
while (τ_current < τ) and (steps_current ≤ steps_max) do
    F_to_prune = bottom_κ(NEXP_map)
    N_pruned(W_pruned) = prune(N_pruned, F_to_prune)
    NEXP_map ← f(X; W_pruned)
    τ_current = FLOPs(N) / FLOPs(N_pruned)
    steps_current ++
end while
return N_pruned(W_pruned)
```

Figure 2: **Pruning YOLOv8m trained on COCO for Object Detection.** Comparative results between neural expressiveness (NEXP) and layer-adaptive magnitude-based pruning method (LAMP) [26]. More comparisons in the supplementary material.

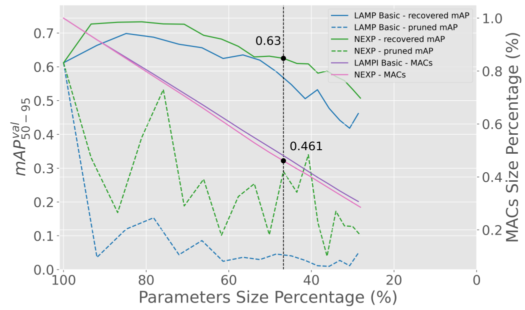

convolutional layer indices, and the y-axis shows feature map indices per layer, standardized through pixel-wise interpolation to align with the layer having the most feature maps. Fig. 1 confirms that NEXP can be effectively estimated using random and limited data samples. Detailed results of this analysis, are presented in Appendix A. The comparative analysis reveals that a mini-batch of 60 samples (0.4% of D in this case) effectively approximates the NEXP scores calculated from the entire dataset, yielding consistent similarity scores above 99% across most similarity metrics (Table. 3).

3.4 Pruning Process

Alg. 1 describes the proposed NEXP-based pruning process, and it has been implemented as extension in the DepGraph pruning framework [11]. A target theoretical speed-up is specified, referred to as the Compression FLOPs Ratio (↓) and denoted by τ. This ratio is calculated using the formula $\frac{\text{original FLOPs}}{\text{compressed FLOPs}}$. To achieve this target ratio, the network may undergo pruning in one or several steps, dictated by the intricacies of the pruning criterion and adjusted according to the quantity of elements removed at each step. For example, NEXP benefits from additional steps, since a filter's score is reliant on its preceding elements (Section 3.2), and a more gradual update on the scores allows for improved pruning precision. A more in-depth analysis of Alg. 1 along with more details on the implementation options are presented in Appendix B.

4 Experimental Evaluation

Details on the experimental settings can be found in Appendix C, including the (a) Datasets and Models (C.1), (b) Adversaries (C.2), (c) Evaluation Metrics (C.3) and (d) Configurations (C.4).

4.1 Comparison w.r.t. State-of-Art Model Compression Strategies

Image Classification on CIFAR-10 and Imagenet-1k. We compare against a plethora of foundational and top-performing approaches, ranging from filter magnitude-based [28, 32, 29] and loss sensitivity-based [58] methods to feature-guided strategies [23, 30] and search algorithms [35, 31].

Outcomes and Discussion. Our findings for various target FLOPs pruning ratios are presented in Tab. 1 (and Tab.6-9 in Appendix D.2) for CIFAR-10, and in Tab. 2 for ImageNet. It is essential to acknowledge the subjectivity in reported performance metrics (accuracy), influenced by the fine-tuning process post-pruning, e.g. the authors in DCP [61] fine-tune for 400 epochs, in contrast to ours 100. We observe that our approach yields consistent improvements in params reduction compared to other methods for given FLOPs ratios, which notably scale significantly for regimes of higher target FLOPs compression ratios τ. For example, on ResNet-56 we show +0.92× average params reduction gains in the 2×-2.20× FLOPs reduction regime, with -0.38%, +0.05% and -0.37% percentage difference in loss respectively to ABC [31], SCP [23] and HRank [30], while on ResNet-110 we

Table 1: Analytical Comparison of Importance-based solutions and Expressiveness on CIFAR-10 using ResNet architectures [17] - ResNet-56 (left) and ResNet-110 (right).

	top-1 acc		Compression Ratio ↓	
Method	Base (%)	Δ (%)	#Params	#FLOPs
L1 [28]	93.06	+0.02	1.16×	1.37×
NEXP (Ours)	93.36	+0.05	**1.69**×	1.53×
GAL-0.6 [32]	93.26	+0.12	1.13×	1.60×
NISP-56 [58]	-	-0.03	1.74×	1.77×
DCP-Adapt [61]	93.80	+0.01	3.37×	1.89×
HRank [30]	93.26	-0.09	1.74×	2.01×
SCP [23]	93.69	-0.46	1.94×	2.06×
NEXP (Ours)	93.36	-0.41	**2.87**×	2.11×
ABC [31]	93.26	-0.03	2.18×	2.18×
NEXP (Ours)	93.36	-1.58	**4.3**×	2.50×
GAL-0.8 [32]	93.26	-1.68	2.93×	2.51×
HRank [30]	93.26	-2.54	3.15×	3.86×
NEXP (Ours)	93.36	-5.12	**21.5**×	5.00×

	top-1 acc		Compression Ratio ↓	
Method	Base (%)	Δ (%)	#Params	#FLOPs
L1 [28]	93.55	+0.02	1.02×	1.19×
NEXP (Ours)	93.79	+0.66	**1.10**×	1.20×
GAL-0.1 [32]	93.50	+0.09	1.04×	1.23×
HRank [30]	93.50	+0.73	1.65×	1.70×
NISP-110 [58]	-	-0.18	1.76×	1.78×
NEXP (Ours)	93.79	+0.18	1.78×	1.80×
GAL-0.5 [32]	93.50	-0.76	1.81×	1.94×
HRank [30]	93.50	-0.14	2.46×	2.39×
NEXP (Ours)	93.79	+0.10	**2.72**×	2.42×
ABC [31]	93.50	+0.08	3.09×	2.87×
NEXP (Ours)	93.79	-0.37	**3.81**×	3.01×
HRank [30]	93.50	-0.85	3.25×	3.19×
NEXP (Ours)	93.79	-0.59	**4.38**×	3.27×

show +1.21× average params reduction gains in the 2.87×-3.27× FLOPs reduction regime, with -0.67% and +0.26% percentage difference in loss respectively to ABC [31] and HRank [30]. Similar observations are evident across all tables, where in certain regimes we also show notable performance gains, up to +1.5%, especially for VGGNet, which is more prone to params reductions due to its plain structure.

Object Detection with YOLOv8. We evaluate expressiveness against four importance based methods, i.e layer-adaptive magnitude-based pruning (LAMP) [26], network slimming (SLIM) [35], Wang's et al. proposed method (DepGraph) [11] and random pruning that serves as a generic pruning baseline [3]. The experiments were conducted on the YOLOv8m model version [22], utilizing the DepGraph pruning framework [11] with an iterative pruning schedule of 16 steps, where after each pruning step the model was fine-tuned for 10 epochs using the coco128 dataset.

Outcomes and Discussion. We report the comparative pruning progress of expressiveness versus the baseline methods, i.e. the remaining percentage of the original model in terms of *MACs* and *params* after each pruning step, named MACs Size Percentage (MSP) and Parameters Size Percentage (PSP) respectively, and highlight the mAP^{val}_{50-95} both after pruning (pruned mAP) and fine-tuning (recovered mAP). We observe that expressiveness outperforms the rest of the reported methods across the whole pruning spectrum, as shown in Fig. 2 (more in Appendix D.2), preserving the initial performance of the model for percentage sizes that reach up to 40% (2.5 $\downarrow$) of that of the original model, with less than 0.5% of recovered performance degradation. Our method even achieves a 3% increase in recovered mAP for 46.1% MSP (2.17 $\downarrow$), in comparison to the baselines that showcase weak recovery capabilities after the 60% (1.67 $\downarrow$) mark in both MSP and PSP. This can be attributed to the intrinsic property of expressiveness to maintain network elements that are more robust to information redistribution, in contrast to "important" labeled structures by other methods. In our experimental scenario, that characteristic is further amplified by the iterative pruning format and the higher amount of fine-tuning epochs at each step, in comparison to conventional pruning schedules that fine-tune for 1 epoch after each iteration or perform a unified fine-tuning session after the last pruning iteration. Interestingly, our criterion also demonstrates significant resistance to performance loss after pruning, achieving 18% increased average performance in terms of pruned mAP compared to the importance-based methods. We have empirically observed that expressiveness benefits from increased cardinality in pruning granularity settings, e.g amount of intermediate steps to achieve a given compression ratio. This stems from expressiveness interactive nature of all elements, as also explained in Sec. 3, where smaller pruning steps combined with iterative fine-tuning, enhance pruning precision and allow for "smoother" redistribution of information in a network, thus contributing to the increased resistance to performance deficits after each pruning step.

4.2 Assessing Hybrid Compression space

In this section, we assess the potential efficiency of "hybrid" pruning strategies exploiting the cooperation between importance and expressiveness. We explore the solution space of "hybrid" compression, using a linear combination of importance and neural expressiveness criteria. We guide exploration through the scoring function: $W_{\text{imp}} \cdot \text{IMP} + W_{\text{nexp}} \cdot \text{NEXP}$ and conduct experiments with

Table 2: Analytical Comparison of Importance-based solutions and Expressiveness on ImageNet-1k using ResNet-50 [17].

Method	Base (%) top-1	Base (%) top-5	Δ Acc (%) top-1	Δ Acc (%) top-5	Compression Ratio #Params ↓	Compression Ratio #FLOPs ↓
NISP-50-B [58]	-	-	-0.89	-	1.78×	1.79×
NEXP (Ours)	76.13	92.86	-1.35	-0.93	2.00×	2.02×
ThiNet [37]	72.88	91.14	-1.87	-1.12	2.06×	2.25×
DCP [61]	76.01	92.93	-1.06	-0.56	2.06×	2.25×
ABC [31]	76.01	92.96	-2.49	-1.45	2.27×	2.30×
NEXP (Ours)	76.13	92.86	-6.77	-3.43	**4.05**×	3.04×
GAL-1-joint [32]	76.15	92.87	-6.84	-3.75	2.50×	3.68×
Hrank [30]	76.15	92.87	-7.15	-3.29	3.08×	4.17×

Figure 3: **Linear exploration of the combinatorial space between importance and expressiveness.**

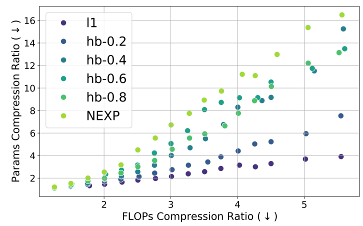

various weight combinations, subject to the constraint $W_{\text{imp}} + W_{\text{nexp}} = 1$. Given that exhaustive search is impractical, we introduce the hyper-parameter $\alpha \in \{0.0, 0.2, \ldots, 0.8, 1.0\}$ to restrict the set of permissible combinations, and modify the constraint to $(1-\alpha) \cdot W_{\text{imp}} + \alpha \cdot W_{\text{nexp}} = 1$. We use group L1-norm [28] as the importance criterion (IMP) and assess all permissible combinations across a linear scale, denoted as τ, representing the target FLOPs compression ratios that we utilized for pruning, on ResNet-56 for CIFAR-10. The outcomes are visualized in Figure 3, which maps our predetermined τ values on the x-axis against the various parameter compression ratios achieved by each combination. Regarding performance, we report the averaged percentage differences in top-1 accuracy between the baseline importance method (L1) and each hybrid format: -0.21% for hb-0.2, -0.96% for hb-0.4, -1.55% for hb-0.6, -1.07% for hb-0.8, and -2.18% for NEXP.

Observations. A consistent pattern is observed across the values of α, where larger values yield higher params compression ratios. Notably, hybrid derivatives allow us to explore sub-spaces with higher parameter compression ratios by sacrificing slight performance accuracy. We also observe that the solution vectors corresponding to IMP and EXP act as extremal points in the solution space of hybrid combinations, thus suggesting a degree of partial orthogonality between the two criteria. Furthermore, the findings reveal a polynomial relationship between parameter compression ratios and FLOPs reduction, with compression ratios increasing polynomially to linear increments in FLOPs reduction, and thus enabling more efficient explorations.

4.3 Evaluating Neural Expressiveness at Initialization

The nature of NEXP allows to be applied in a weight agnostic manner, i.e. on untrained networks. An extended version of the section's 3.3 analysis, which also includes untrained models (Appendix A), reveals that $NEXP_{\text{map}}$'s obtained at initialization and after network convergence share some expressiveness pattern similarities, particularly in the initial layers. Our numeric evaluation shows a notable correlation between the initialization and converged states for DenseNet-40 and VGG-19, with cosine similarities of 84.10% and 86.82%, respectively. It also indicates greater consistency in neural expressiveness measurements for the first layers of all networks, which could be considered important for the formation of critical paths [2]. Motivated by these observations, we also assess the efficacy of expressiveness as criterion for Pruning at Initialization against various SOTA approaches [27, 50, 46] (Appendix D.1). Our method consistently outperforms (in terms of top-1 acc) all other algorithms, particularly in regimes of lower compression, up to $10^2(\downarrow)$ with an average increase of 1.21% over SynFlow, while maintaining competitiveness at higher compression levels, above $10^2(\downarrow)$ with an average percentage difference of 4.82%, 3.72% and -2.74%, compared to [50], [27] and [46]. In summary, under the assumption that the selection of hyperparameters remains congruent with the initialization [12], consistent map measurements between initial and final states can effectively evaluate NEXP's ability to identify winning tickets. However, a robust evaluation should also consider the initial state quality and the training process, while addressing the "When to prune" question [42].

5 Conclusions

In this work, we have introduced "Neural Expressiveness" as a new criterion for model compression. In our NEXP steps, we will explore optimal solutions for the "When" and "How" to prune questions.

References

[1] Armstrong Aboah, Bin Wang, Ulas Bagci, and Yaw Adu-Gyamfi. Real-time multi-class helmet violation detection using few-shot data sampling technique and yolov8. In *Proceedings of the IEEE/CVF Conference on Computer Vision and Pattern Recognition (CVPR) Workshops*, pages 5350–5358, June 2023.

[2] Alessandro Achille, Matteo Rovere, and Stefano Soatto. Critical learning periods in deep networks. In *International Conference on Learning Representations*, 2019.

[3] Davis Blalock, Jose Javier Gonzalez Ortiz, Jonathan Frankle, and John Guttag. What is the state of neural network pruning? In I. Dhillon, D. Papailiopoulos, and V. Sze, editors, *Proceedings of Machine Learning and Systems*, volume 2, pages 129–146, 2020.

[4] Miguel Á. Carreira-Perpiñán and Yerlan Idelbayev. "learning-compression" algorithms for neural net pruning. In *Proceedings of the IEEE Conference on Computer Vision and Pattern Recognition (CVPR)*, June 2018.

[5] Y Chen, Tien-Ju Yang, Joel Emer, and Vivienne Sze. Understanding the limitations of existing energy-efficient design approaches for deep neural networks. *Energy*, 2(L1):L3, 2018.

[6] I. Daubechies, M. Defrise, and C. De Mol. An iterative thresholding algorithm for linear inverse problems with a sparsity constraint. *Communications on Pure and Applied Mathematics*, 57(11):1413–1457, 2004.

[7] Lei Deng, Guoqi Li, Song Han, Luping Shi, and Yuan Xie. Model compression and hardware acceleration for neural networks: A comprehensive survey. *Proceedings of the IEEE*, 108(4):485–532, 2020.

[8] Xiaohan Ding, guiguang ding, Xiangxin Zhou, Yuchen Guo, Jungong Han, and Ji Liu. Global sparse momentum sgd for pruning very deep neural networks. In H. Wallach, H. Larochelle, A. Beygelzimer, F. d'Alché-Buc, E. Fox, and R. Garnett, editors, *Advances in Neural Information Processing Systems*, volume 32. Curran Associates, Inc., 2019.

[9] Tausif Diwan, G Anirudh, and Jitendra V Tembhurne. Object detection using yolo: Challenges, architectural successors, datasets and applications. *multimedia Tools and Applications*, 82(6):9243–9275, 2023.

[10] Andrei Dumitriu, Florin Tatui, Florin Miron, Radu Tudor Ionescu, and Radu Timofte. Rip current segmentation: A novel benchmark and yolov8 baseline results. In *Proceedings of the IEEE/CVF Conference on Computer Vision and Pattern Recognition (CVPR) Workshops*, pages 1261–1271, June 2023.

[11] Gongfan Fang, Xinyin Ma, Mingli Song, Michael Bi Mi, and Xinchao Wang. Depgraph: Towards any structural pruning. In *Proceedings of the IEEE/CVF Conference on Computer Vision and Pattern Recognition (CVPR)*, pages 16091–16101, June 2023.

[12] Jonathan Frankle and Michael Carbin. The lottery ticket hypothesis: Finding sparse, trainable neural networks, 2019.

[13] Yiwen Guo, Anbang Yao, and Yurong Chen. Dynamic network surgery for efficient dnns. In D. Lee, M. Sugiyama, U. Luxburg, I. Guyon, and R. Garnett, editors, *Advances in Neural Information Processing Systems*, volume 29. Curran Associates, Inc., 2016.

[14] Song Han, Huizi Mao, and William J. Dally. Deep compression: Compressing deep neural networks with pruning, trained quantization and huffman coding, 2016.

[15] Song Han, Jeff Pool, John Tran, and William Dally. Learning both weights and connections for efficient neural network. In C. Cortes, N. Lawrence, D. Lee, M. Sugiyama, and R. Garnett, editors, *Advances in Neural Information Processing Systems*, volume 28. Curran Associates, Inc., 2015.

[16] Babak Hassibi and David Stork. Second order derivatives for network pruning: Optimal brain surgeon. In S. Hanson, J. Cowan, and C. Giles, editors, *Advances in Neural Information Processing Systems*, volume 5. Morgan-Kaufmann, 1992.

[17] Kaiming He, Xiangyu Zhang, Shaoqing Ren, and Jian Sun. Deep residual learning for image recognition. In *Proceedings of the IEEE Conference on Computer Vision and Pattern Recognition (CVPR)*, June 2016.

[18] Andrew Howard, Andrey Zhmoginov, Liang-Chieh Chen, Mark Sandler, and Menglong Zhu. Inverted residuals and linear bottlenecks: Mobile networks for classification, detection and segmentation. In *CVPR*, 2018.

[19] Andrew G. Howard, Menglong Zhu, Bo Chen, Dmitry Kalenichenko, Weijun Wang, Tobias Weyand, Marco Andreetto, and Hartwig Adam. Mobilenets: Efficient convolutional neural networks for mobile vision applications, 2017.

[20] Hengyuan Hu, Rui Peng, Yu-Wing Tai, and Chi-Keung Tang. Network trimming: A data-driven neuron pruning approach towards efficient deep architectures, 2016.

[21] Gao Huang, Zhuang Liu, Laurens van der Maaten, and Kilian Q. Weinberger. Densely connected convolutional networks. In *Proceedings of the IEEE Conference on Computer Vision and Pattern Recognition (CVPR)*, July 2017.

[22] Glenn Jocher, Ayush Chaurasia, and Jing Qiu. Ultralytics yolov8, 2023.

[23] Minsoo Kang and Bohyung Han. Operation-aware soft channel pruning using differentiable masks. In Hal Daumé III and Aarti Singh, editors, *Proceedings of the 37th International Conference on Machine Learning*, volume 119 of *Proceedings of Machine Learning Research*, pages 5122–5131. PMLR, 13–18 Jul 2020.

[24] Alex Krizhevsky, Geoffrey Hinton, et al. Learning multiple layers of features from tiny images. Technical report, 2009.

[25] Yann LeCun, John Denker, and Sara Solla. Optimal brain damage. In D. Touretzky, editor, *Advances in Neural Information Processing Systems*, volume 2. Morgan-Kaufmann, 1989.

[26] Jaeho Lee, Sejun Park, Sangwoo Mo, Sungsoo Ahn, and Jinwoo Shin. Layer-adaptive sparsity for the magnitude-based pruning, 2021.

[27] Namhoon Lee, Thalaiyasingam Ajanthan, and Philip H. S. Torr. Snip: Single-shot network pruning based on connection sensitivity, 2019.

[28] Hao Li, Asim Kadav, Igor Durdanovic, Hanan Samet, and Hans Peter Graf. Pruning filters for efficient convnets, 2017.

[29] Yuchao Li, Shaohui Lin, Baochang Zhang, Jianzhuang Liu, David Doermann, Yongjian Wu, Feiyue Huang, and Rongrong Ji. Exploiting kernel sparsity and entropy for interpretable cnn compression. In *Proceedings of the IEEE/CVF Conference on Computer Vision and Pattern Recognition (CVPR)*, June 2019.

[30] Mingbao Lin, Rongrong Ji, Yan Wang, Yichen Zhang, Baochang Zhang, Yonghong Tian, and Ling Shao. Hrank: Filter pruning using high-rank feature map. In *Proceedings of the IEEE/CVF Conference on Computer Vision and Pattern Recognition (CVPR)*, June 2020.

[31] Mingbao Lin, Rongrong Ji, Yuxin Zhang, Baochang Zhang, Yongjian Wu, and Yonghong Tian. Channel pruning via automatic structure search. *arXiv preprint arXiv:2001.08565*, 2020.

[32] Shaohui Lin, Rongrong Ji, Chenqian Yan, Baochang Zhang, Liujuan Cao, Qixiang Ye, Feiyue Huang, and David Doermann. Towards optimal structured cnn pruning via generative adversarial learning. In *Proceedings of the IEEE/CVF Conference on Computer Vision and Pattern Recognition (CVPR)*, June 2019.

[33] Tsung-Yi Lin, Michael Maire, Serge Belongie, James Hays, Pietro Perona, Deva Ramanan, Piotr Dollár, and C. Lawrence Zitnick. Microsoft COCO: Common Objects in Context. In David Fleet, Tomas Pajdla, Bernt Schiele, and Tinne Tuytelaars, editors, *Computer Vision – ECCV 2014*, Lecture Notes in Computer Science, pages 740–755, Cham, 2014. Springer International Publishing.

[34] Tantan Liu and Gagan Agrawal. Stratified k-means clustering over a deep web data source. In *Proceedings of the 18th ACM SIGKDD international conference on Knowledge discovery and data mining*, pages 1113–1121, 2012.

[35] Zhuang Liu, Jianguo Li, Zhiqiang Shen, Gao Huang, Shoumeng Yan, and Changshui Zhang. Learning efficient convolutional networks through network slimming, 2017.

[36] Zhuang Liu, Mingjie Sun, Tinghui Zhou, Gao Huang, and Trevor Darrell. Rethinking the value of network pruning, 2019.

[37] Jian-Hao Luo, Jianxin Wu, and Weiyao Lin. Thinet: A filter level pruning method for deep neural network compression. In *Proceedings of the IEEE International Conference on Computer Vision (ICCV)*, Oct 2017.

[38] Pavlo Molchanov, Arun Mallya, Stephen Tyree, Iuri Frosio, and Jan Kautz. Importance estimation for neural network pruning. In *Proceedings of the IEEE/CVF Conference on Computer Vision and Pattern Recognition (CVPR)*, June 2019.

[39] Sumit Pandey, Kuan-Fu Chen, and Erik B. Dam. Comprehensive multimodal segmentation in medical imaging: Combining yolov8 with sam and hq-sam models. In *Proceedings of the IEEE/CVF International Conference on Computer Vision (ICCV) Workshops*, pages 2592–2598, October 2023.

[40] Olga Russakovsky, Jia Deng, Hao Su, Jonathan Krause, Sanjeev Satheesh, Sean Ma, Zhiheng Huang, Andrej Karpathy, Aditya Khosla, Michael Bernstein, Alexander C. Berg, and Li Fei-Fei. ImageNet Large Scale Visual Recognition Challenge. *International Journal of Computer Vision*, 115(3):211–252, December 2015.

[41] Victor Sanh, Thomas Wolf, and Alexander Rush. Movement pruning: Adaptive sparsity by fine-tuning. In H. Larochelle, M. Ranzato, R. Hadsell, M.F. Balcan, and H. Lin, editors, *Advances in Neural Information Processing Systems*, volume 33, pages 20378–20389. Curran Associates, Inc., 2020.

[42] Maying Shen, Pavlo Molchanov, Hongxu Yin, and Jose M. Alvarez. When to prune? a policy towards early structural pruning. In *Proceedings of the IEEE/CVF Conference on Computer Vision and Pattern Recognition (CVPR)*, pages 12247–12256, June 2022.

[43] Karen Simonyan and Andrew Zisserman. Very deep convolutional networks for large-scale image recognition, 2015.

[44] Karen Simonyan and Andrew Zisserman. Very Deep Convolutional Networks for Large-Scale Image Recognition, April 2015. arXiv:1409.1556 [cs].

[45] Christian Szegedy, Wei Liu, Yangqing Jia, Pierre Sermanet, Scott Reed, Dragomir Anguelov, Dumitru Erhan, Vincent Vanhoucke, and Andrew Rabinovich. Going deeper with convolutions. In *Proceedings of the IEEE Conference on Computer Vision and Pattern Recognition (CVPR)*, June 2015.

[46] Hidenori Tanaka, Daniel Kunin, Daniel L Yamins, and Surya Ganguli. Pruning neural networks without any data by iteratively conserving synaptic flow. In H. Larochelle, M. Ranzato, R. Hadsell, M. F. Balcan, and H. Lin, editors, *Advances in Neural Information Processing Systems*, volume 33, pages 6377–6389. Curran Associates, Inc., 2020.

[47] Lucas Theis, Iryna Korshunova, Alykhan Tejani, and Ferenc Huszár. Faster gaze prediction with dense networks and fisher pruning, 2018.

[48] Neil C. Thompson, Kristjan Greenewald, Keeheon Lee, and Gabriel F. Manso. The computational limits of deep learning, 2022.

[49] Sunil Vadera and Salem Ameen. Methods for pruning deep neural networks. *IEEE Access*, 10:63280–63300, 2022.

[50] Chaoqi Wang, Guodong Zhang, and Roger Grosse. Picking winning tickets before training by preserving gradient flow, 2020.

[51] Qing Ren Wang and Ching Y. Suen. Analysis and design of a decision tree based on entropy reduction and its application to large character set recognition. *IEEE Transactions on Pattern Analysis and Machine Intelligence*, PAMI-6(4):406–417, 1984.

[52] Shiqiang Wang. Efficient deep learning. *Nature Computational Science*, 1(3):181–182, March 2021. Number: 3 Publisher: Nature Publishing Group.

[53] Bichen Wu, Alvin Wan, Xiangyu Yue, Peter Jin, Sicheng Zhao, Noah Golmant, Amir Gholaminejad, Joseph Gonzalez, and Kurt Keutzer. Shift: A zero flop, zero parameter alternative to spatial convolutions. In *Proceedings of the IEEE Conference on Computer Vision and Pattern Recognition (CVPR)*, June 2018.

[54] Kaixin Xu, Zhe Wang, Xue Geng, Min Wu, Xiaoli Li, and Weisi Lin. Efficient joint optimization of layer-adaptive weight pruning in deep neural networks. In *Proceedings of the IEEE/CVF International Conference on Computer Vision (ICCV)*, pages 17447–17457, October 2023.

[55] Pengtao Xu, Jian Cao, Fanhua Shang, Wenyu Sun, and Pu Li. Layer pruning via fusible residual convolutional block for deep neural networks, 2020.

[56] Tien-Ju Yang, Yu-Hsin Chen, and Vivienne Sze. Designing energy-efficient convolutional neural networks using energy-aware pruning. In *Proceedings of the IEEE Conference on Computer Vision and Pattern Recognition (CVPR)*, July 2017.

[57] Jiecao Yu, Andrew Lukefahr, David Palframan, Ganesh Dasika, Reetuparna Das, and Scott Mahlke. Scalpel: Customizing dnn pruning to the underlying hardware parallelism. In *Proceedings of the 44th Annual International Symposium on Computer Architecture*, ISCA '17, page 548–560, New York, NY, USA, 2017. Association for Computing Machinery.

[58] Ruichi Yu, Ang Li, Chun-Fu Chen, Jui-Hsin Lai, Vlad I. Morariu, Xintong Han, Mingfei Gao, Ching-Yung Lin, and Larry S. Davis. Nisp: Pruning networks using neuron importance score propagation. In *Proceedings of the IEEE Conference on Computer Vision and Pattern Recognition (CVPR)*, June 2018.

[59] Xiangyu Zhang, Xinyu Zhou, Mengxiao Lin, and Jian Sun. Shufflenet: An extremely efficient convolutional neural network for mobile devices. In *Proceedings of the IEEE Conference on Computer Vision and Pattern Recognition (CVPR)*, June 2018.

[60] Zhengguang Zhou, Wengang Zhou, Houqiang Li, and Richang Hong. Online filter clustering and pruning for efficient convnets. In *2018 25th IEEE International Conference on Image Processing (ICIP)*, pages 11–15, 2018.

[61] Zhuangwei Zhuang, Mingkui Tan, Bohan Zhuang, Jing Liu, Yong Guo, Qingyao Wu, Junzhou Huang, and Jinhui Zhu. Discrimination-aware Channel Pruning for Deep Neural Networks. In S. Bengio, H. Wallach, H. Larochelle, K. Grauman, N. Cesa-Bianchi, and R. Garnett, editors, *Advances in Neural Information Processing Systems*, volume 31. Curran Associates, Inc., 2018.

A Duality of Independence: Data (X) and Information State (W_{t_i})

Fig. 4 presents a detailed comparative illustration that highlights the similarities in NEXP estimations across various networks, including VGGNet [44], ResNet [17], MobileNet [19] and DenseNet [21] on CIFAR-10 dataset. Specifically, for each network architecture, we showcase expressiveness distributions in both untrained (PaI) and trained (PaT) states. In each sub-figure, the x-axis indicates convolutional layer indices, and the y-axis shows feature map indices per layer, standardized through pixel-wise interpolation to align with the layer having the most feature maps. Columns represent various sampling strategies, while colors indicate expressiveness levels, with higher values signifying greater expressiveness. In other words, the figure illustrates a two-fold sensitivity analysis of NEXP to (i) the mini-batch data (X, as outlined in Alg. 1), using two input sampling strategies to assemble a batch with 60 samples, namely random sampling (denoted as 'random') and class-representative sampling via k-means (denoted as 'k-means'), and (ii) the information state (W_{t_i}), specifically comparing expressiveness at initialization (PaI) against expressiveness after training (PaT), when weights have converged.

A.1 True NEXP value (non-approx).

We define the true NEXP score for each filter as the value obtained by comparing all activation patterns across the entire training dataset D. In that way, the ability of each element to extract maximal features is evaluated for every data-point in the input feature space of a task at hand. In this study however, due to GPU memory constraints (limited to 12GB of GDDR6 SDRAM), we employed 25% of the total training set, ensuring class distribution is preserved, to determine these exact NEXP scores, denoted as non-approx.

A.2 Data Agnostic.

To evaluate NEXP's sensitivity to input data, we conduct a similarity analysis for each row in Fig. 4. For each information state (PaI and PaT), we compare the expressiveness map ($NEXP_{\text{map}}$) derived from each sampling strategy against the true NEXP values (non-approx), corresponding to each respective state. For a comprehensive comparison, we utilize various similarity metrics, such as Euclidean Distance, Cosine Similarity, Pearsonr Similarity, and the Structural Similarity Index Measure (ssim_index). Detailed results of this analysis, specific to each state, are presented in Tables 3 (PaT) and 4 (PaI). The comparative analysis reveals that a mini-batch of 60 samples, with a balanced representation from each class, effectively approximates the NEXP scores calculated from the entire dataset, yielding consistent similarity scores above 99% across all similarity metrics for both PaI and PaT. Interestingly, random sampling consistently outperforms the k-means selection strategy, which involves selecting 6 representative samples per CIFAR-10 class. This is especially notable in PaT, with random sampling showing up to a 7.51% higher Pearson correlation, 5% improvement in ssim_index, and 1.14 reduction in Euclidean distance compared to k-means. This further reinforces the statement that comparing activation patterns reflects the intrinsic ability of neural networks to distinguish various input spaces, thus effectively extending the NEXP criterion to random input data and laying the foundation for investigating *Data-Agnostic strategies*.

A.3 Weight Agnostic

Fig. 4 reveals that $NEXP_{\text{map}}$'s obtained at initialization and after network convergence share some expressiveness pattern similarities, particularly in the initial layers. Detailed comparisons of these similarities across all layers, and specifically for the first five, are presented in Table 5, contrasting the initial maps with the true $NEXP_{\text{map}}$ post-training. The summary of our numeric evaluation confirms a notable correlation between the initialization and converged states for DenseNet-40 and VGG-19, showing up to 84.10% and 86.82% in cosine similarity respectively. It also indicates greater consistency in neural expressiveness measurements for the first layers of all networks, which could be considered important for the formation of critical paths. In this context, the formation of the final state depends on hyperparameter choices, like weight decay and learning rate, and the stochastic nature of training, that could potentially alter the model's progression from its initial state, as also highlighted by Frankle et al. [12]. In that manner, under the assumption that the selection of hyperparameters remains congruent with the initialization, "Expressiveness" can be considered a fit criterion for Pruning at Initialization (PaI). In summary, the consistency of map measurements between initial and final states may serve as a solid metric for evaluating NEXP's ability to identify winning tickets. Nevertheless, a more robust process of its evaluation should also take into account the quality of the initial state as well as the subsequent training process.

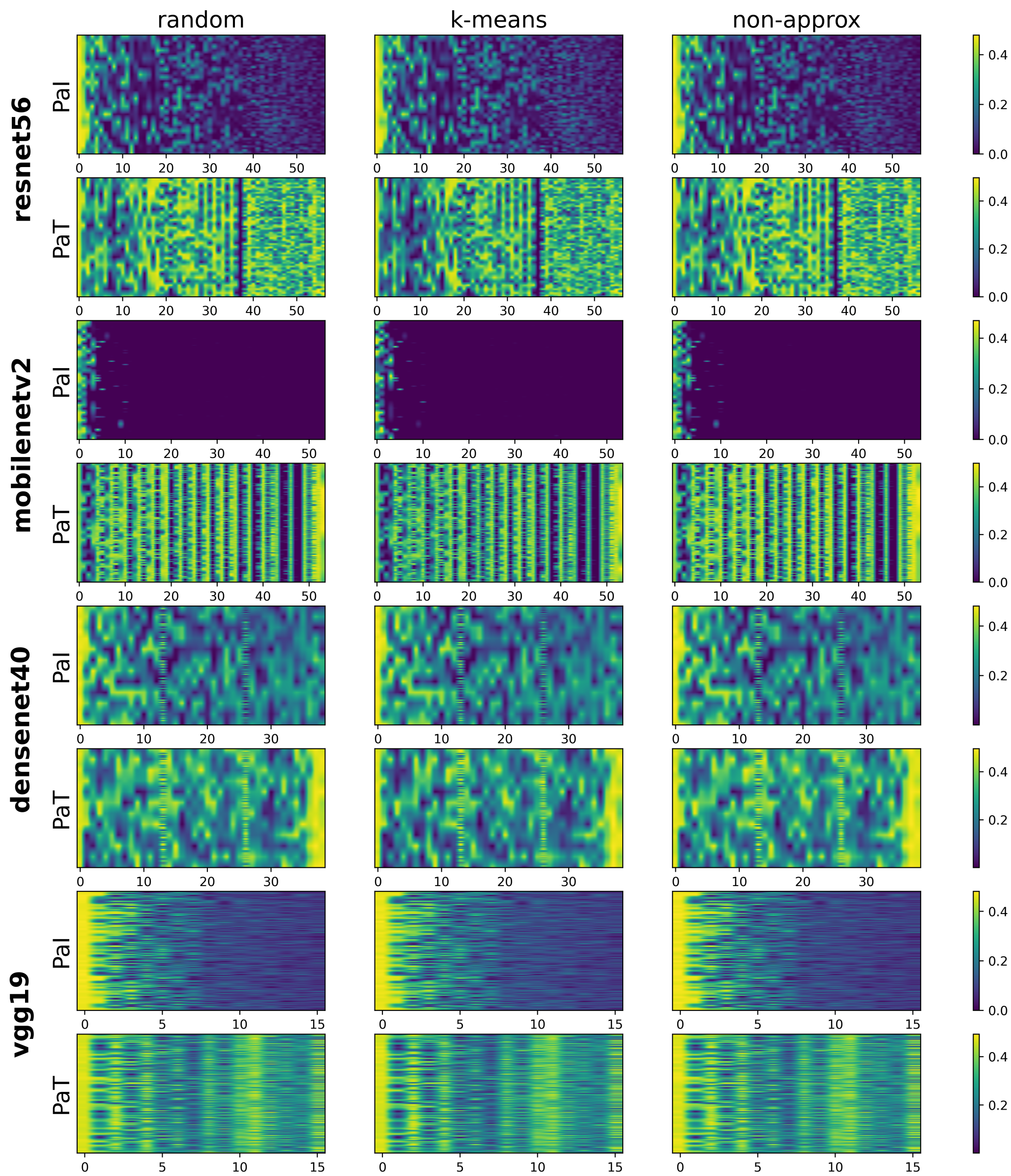

Figure 4: **Expressiveness statistics of feature maps from different convolutional layers and architectures on CIFAR-10 (Extended).** For each architecture we demonstrate the expressiveness distribution for both an untrained instance of the model (PaI), as well as a converged one (PaT). The x-axis represents the indices of convolutional layers and y-axis that of the feature maps in each layer. To maintain consistency across the y-axis, we have interpolated each layer's feature maps (pixel-wise) to match the layer with the most feature maps. Columns denote different sampling strategies and different colors denote different expressiveness values (the higher the value, the more expressive the feature map). To approximate the expressiveness score of each element, denoted as "non-approx", we used 25% of all dataset's samples (not 100% due to memory limitations) maintaining the label's distribution. As can be seen, the rank of each feature map (column of the sub-figure) is almost unchanged (the same color), regardless of the image batches. Hence, even a small number of images can effectively estimate the average rank of each feature map in different architectures.

Table 3: Sensitivity analysis of the input's sampling strategies after training (PaT) using various similarity metrics.

Model	Sampling Strategy	Euclidean Distance	Cosine Similarity	Pearsonr Similarity	ssim_index
ResNet-56 [17]	random	**0.2349**	**0.9998**	-	**0.9979**
	k-means	1.3729	0.9949	-	0.9479
MobileNet-v2 [19]	random	**0.2903**	**0.9994**	**0.9810**	**0.9988**
	k-means	1.1197	0.9960	0.9059	0.9794
DenseNet-40 [21]	random	**0.2751**	**0.9997**	**0.9818**	**0.9970**
	k-means	1.1669	0.9959	0.9527	0.9614
VGG-19 [44]	random	**0.5150**	**0.9989**	**0.9814**	**0.9894**
	k-means	0.8438	0.9964	0.9556	0.9728

Table 4: Sensitivity analysis of the input's sampling strategies at Initialization (PaI) using various similarity metrics.

Model	Sampling Strategy	Euclidean Distance	Cosine Similarity	Pearsonr Similarity	ssim_index
ResNet-56 [17]	random	**0.1333**	**0.9996**	**0.9979**	**0.9984**
	k-means	0.3948	0.9984	0.9868	0.9859
MobileNet-v2 [19]	random	**0.0340**	**0.9565**	-	**0.9994**
	k-means	0.2441	0.9454	-	0.9776
DenseNet-40 [21]	random	**0.2297**	**0.9997**	0.9927	**0.9977**
	k-means	0.2972	0.9994	**0.9941**	0.9955
VGG-19 [44]	random	**0.2688**	**0.9988**	0.9652	**0.9950**
	k-means	0.4882	0.9975	**0.9724**	0.9856

Table 5: Sensitivity analysis of $NEXP_{\text{map}}$'s retrieved at initialization compared with the true $NEXP_{\text{map}}$ following model convergence.

Model	Metric	random		k-means		non-approx (PaI)	
		All	first-5	All	first-5	All	first-5
ResNet-56 [17]	Euclidean Distance	9.0326	5.2005	**8.8029**	**5.1177**	8.9986	5.1850
	Cosine Similarity	0.7584	0.8765	**0.7677**	**0.8784**	0.7592	0.8751
	ssim_index	0.0194	0.3794	**0.0243**	**0.3990**	0.0206	0.3810
MobileNet-v2 [19]	Euclidean Distance	**10.5470**	**7.4966**	10.6056	8.0843	10.5492	7.5134
	Cosine Similarity	0.4645	**0.6478**	0.4910	0.5862	**0.6702**	0.6461
	ssim_index	-0.0018	**0.1187**	-0.0011	0.0942	-0.0020	0.1142
DenseNet-40 [21]	Euclidean Distance	6.1326	**4.6957**	**6.0594**	4.7157	6.1043	4.7364
	Cosine Similarity	0.8357	**0.8769**	**0.8410**	0.8762	0.8378	0.8761
	ssim_index	**0.0169**	**0.4552**	0.0101	0.4493	0.0150	0.4464
VGG-19 [44]	Euclidean Distance	6.3171	4.9532	**6.1194**	**4.8525**	6.3083	4.9810
	Cosine Similarity	0.8610	0.8979	**0.8682**	**0.9030**	0.8624	0.8972
	ssim_index	0.0808	0.3798	**0.0812**	**0.3844**	0.0808	0.3712

B Pruning Process: An in-depth analysis

B.1 Global vs local -scope pruning.

NEXP is used in the pruning process to evaluate and rank different network elements, guiding their subsequent removal based on their scores. In our study, we focused on the removal of filters, i.e., Filter Pruning, where we pruned convolutional structures by removing the least expressive filters. This can be approached in two ways: (i) on a local (layer-by-layer) basis, where filters are assessed and removed according to their expressiveness relative to other filters within the same layer, e.g., eliminating the least μ expressive filters from each layer. (ii) On a global (network-wide) basis, where all filters across layers are normalized in terms of their scores, allowing for the removal of the least κ expressive filters from the entire network. We experimentally observed that “Global Pruning" yields consistent results and outperforms “Local Pruning" when using the NEXP pruning criterion. Therefore, all the experiments reported in this paper were conducted using the “Global Pruning" approach.

B.2 One-shot vs Iterative pruning.

Furthermore, another design parameter to consider in the pruning process is its coordination with fine-tuning. In this context, two widely adopted strategies are: (a) “One-Shot" pruning, where pruning is completed entirely before any fine-tuning occurs, and (b) “Iterative" pruning, which involves alternating between pruning and fine-tuning via an iterative sequence. The first one (a) can be considered a more lightweight approach and allows for a more robust evaluation of the pruning metric at hand, when compared to the later one (b). This is because it has no extra dependency on the training data and its efficiency does not depend on the iterative re-calibration of the information state through the fine-tuning process. In this study, most experiments where conducted using “One-Shot" pruning, while we also explored the integration of NEXP in an “Iterative" pruning process with YOLOv8 (more details on 4.1), where we noted a reduction in performance declines and an improvement in the performance recovery after each pruning step, leading to better overall results.

B.3 Detailed description of all algorithmic steps.

More in detail regarding Algorithm 1, we define the data structure $NEXP_{\text{map}}$, i.e., a dictionary in our implementation, to store the NEXP scores for every filter in the neural network after each iteration. Given a neural network $\mathcal{N}$ with its current weight state W_{t_i}, we initially set up all variables required for the pruning loop (Lines 1-4). The network is then gradually pruned until one of the following conditions is met: the target ratio is achieved or the allowed number of pruning steps is exceeded (Line 5). During each pruning iteration, the κ least expressive filters from the current pruned state of the network are initially selected (Line 6). These filters are then removed, followed by an update to $NEXP_{\text{map}}$ for the subsequent iteration (Lines 7-8). To obtain the NEXP scores, a forward pass $f(X; W_{\text{pruned}})$ is conducted using a user-provided mini-batch as input. Finally, the conditions variables are updated in preparation for the next pruning iteration (Lines 9-10).

B.4 Acceleration of NEXP computations.

In Algorithm 1, Line 8 accounts for the bulk of the computational complexity. Specifically, the calculation of $NEXP_{\text{map}}$ can be divided into two sub-processes: (i) performing a forward pass to retrieve all activation patterns, and (ii) estimating the NEXP score for each element in the map. However, performing a forward pass can be considered negligible compared to computing the NEXP score for each filter. This is because the later involves multiple comparisons between the activation patterns of all samples in the mini-batch X for every filter. Two effective ways to reduce this computational demand are: first, all operations involved in computing the NEXP score are compatible with widely-used BLAS libraries, facilitating hardware acceleration; second, the frequency of score updates can be strategically decreased under certain conditions, e.g., every n pruning iterations.

C Experimental Settings

C.1 Datasets and Models.

This paper explores Computer Vision tasks through extensive experiments on various datasets, such as CIFAR-10 [24] and ImageNet [40] for image classification, and COCO [33] for object detection. To demonstrate the robustness of our approach, we experiment on several popular architectures and a wide span of architectural elements, including VGGNet with a plain structure [44], ResNet with a residual structure [17], GoogLeNet with inception modules [45], MobileNet with depthwise separable convolutions [19], DenseNet with dense blocks [21] and YOLOv8 with a variety of different modules, e.g. C2f and SPPF [22].

C.2 Adversaries.

We assess the efficacy of expressiveness as criterion for Pruning both after Training (PaT) and at Initialization (PaI), using arbitrary (random) data-points. For PaT (4.1), we compare against a plethora of foundational and state-of-the-art approaches, ranging from filter magnitude-based [28, 32, 29] and loss sensitivity-based [58] methods to feature-guided strategies [23, 30] and search algorithms [35, 31]. Regarding PaI (4.3 and D.1), our comparison is two-fold, as we evaluate expressiveness using (i) single-shot and (ii) iterative pruning. More specifically, the adversaries for PaI include pruning with random scoring, two state-of-the-art single-shot pruning strategies, namely SNIP [27] and GraSP [50], as well as one state-of-the-art iterative pruning strategy, named SynFlow [46].

C.3 Evaluation Metrics.

To effectively quantify the efficiency of reported solutions, we adopt a 3-dimensional evaluation space, consisting of i) two widely-used metrics i.e. *FLOPs* and *params*, that define the 2-dimensional compression solution efficiency, alongside with ii) an NN model accuracy to assess the predictions of pruned derivatives [3]. Within the compression space, we define, (a) Compression Ratio($\downarrow$) $= \frac{\text{original size}}{\text{compressed size}}$ and (b) Compressed Size Percentage (%) $= \frac{\text{compressed size}}{\text{original size}} \cdot 100$. To assess task-specific capabilities, we report the top-1 accuracy of pruned models for image classification on CIFAR-10 [24], both top-1 and top-5 accuracies for ImageNet [40], and the mean Average Precision (mAP) over IoU (Intersection over Union) thresholds ranging from 0.5 to 0.95, denoted as mAP^{val}_{50-95}, for object detection on the COCO dataset [33].

C.4 Configurations.

We implement the proposed “expressiveness" pruning criterion on PyTorch, version 2.0.1+cu117, by extending the DepGraph pruning framework [11] to maintain models compatibility and to ensure structural coupling during the removal of network elements e.g., simultaneously removing any inter-dependent network elements such as kernel pairs of convolutional and batch-normalization batched layers. All experiments are conducted on a NVIDIA GeForce RTX 3060 GPU with 12GB of GDDR6 SDRAM. For all experiments we use a batch of 64 random data-points to estimate expressiveness, except those that are reported for CIFAR-10 and ImageNet on 4.1, where we used K-Means to select 60 samples (6 from each class). Additionally, the baseline models on CIFAR-10 were trained for 200 epochs by using 128 batch size and Stochastic Gradient Descent algorithm (SGD) with an initial learning rate of 0.1 that is divided by 10 after 60 and 120 epochs respectively. For ImageNet models and YOLOv8, we utilize the available pre-trained weights on PyTorch vision library and ultralytics [22]. We fine-tune the pruned networks for 100 epochs on CIFAR-10 and for 30 epochs on ImageNet to compensate for the performance loss, using a batch size of 128 and 32 respectively.

D Supplementary Experimental Results

D.1 Neural Expressiveness at Initialization: A comparative study

Adversaries. We establish our comparative study in a two-fold manner, as we compare expressiveness against (i) single-shot and (ii) iterative pruning approaches. More specifically, the adversaries include pruning with random scoring, two state-of-the-art single-shot pruning strategies, namely SNIP [27] and GraSP [50], as well as one state-of-the-art iterative pruning strategy, named SynFlow [46]. For our approach, we implement one-shot pruning, utilizing a batch of 64 arbitrary data points for the estimation of expressiveness.

Experimental Setup. We adopt the experimental framework of Tanaka et al. [46], who assess algorithm performance across an exponential scale (10^r) of parameters compression ratios $r \in \{0.00, 0.25, 0.50, 0.75, \dots\}$. Their proposed settings also enable for the evaluation of an algorithm's resilience to "layer collapses", typically observed at higher compression levels. **Results.** We prune VGG-16 on CIFAR-10 and compare against the findings of [46]. We remain consistent with our adversaries and train the model for 160 epochs, using a batch size of 128 and an initial learning rate of 0.1, which is reduced by a factor of 10 after 60 and 120 epochs. The results are illustrated on Fig. 5.

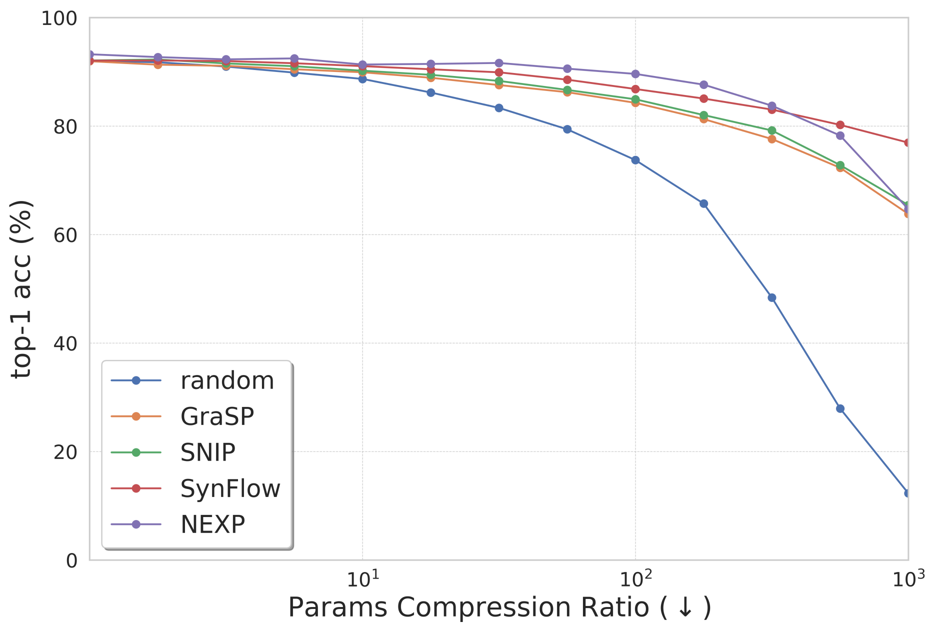

Figure 5: **Pruning VGG-16 at Initialization on CIFAR-10.** A comparative visualisation of SOTA methods across an exponential scale of params compression ratios.

Observations. Our method consistently outperforms all other algorithms, particularly in regimes of lower compression, up to $10^2(\downarrow)$ with an average increase of 1.21% over SynFlow, while maintaining competitiveness at higher compression levels, above $10^2(\downarrow)$ with an average percentage difference of 4.82%, 3.72% and -2.74%, compared to GraSP, SNIP and SynFlow respectively.

D.2 Additional Experimental Results: Tables and Figures

CIFAR-10. We present further experiments and comparisons with state-of-the-art methods, including HRANK [30], GAL [32], ABC [31] and DCP [61], specifically for GoogLeNet and MobileNet-v2 networks. For MobileNet-v2, our method attains an increased compression ratio of $0.94\times$ in parameters and $0.75\times$ in FLOPs ($\downarrow$), with a minimal decrease of only -0.09% in performance compared to DCP. In the GoogLeNet case, we demonstrate a notable enhancement in parameters compression within the $1.60\times$ to $2.20\times$ FLOPs compression range, surpassing GAL and HRANK with margins of $1.8\times$ and $1.52\times$ respectively, with an average improvement of 7.5% in performance degradation.

Table 6: Analytical Comparison of Importance-based solutions and Expressiveness on CIFAR-10 using VGGNet architectures [44].

Model	Method	top-1 acc Base (%)	Δ (%)	Compression Ratio ↓ #Params	#FLOPs
VGG-16	L1 [28]	93.25	+0.15	2.78×	1.52×
	GAL-0.05 [32]	93.96	-0.19	4.46×	1.65×
	GAL-0.1 [32]		-0.54	5.61×	1.82×
	HRank [30]	93.96	-0.53	5.97×	2.15×
	HRank [30]	93.96	-1.62	5.67×	2.89×
	SCP [23]	93.85	-0.06	15.38×	2.96×
	NEXP (Ours)	93.87	-0.16	5.62×	3.03×
	ABC [31]	93.02	+0.06	8.80×	3.80×
	NEXP (Ours)	93.87	-0.35	**13.13**×	4.01×
	HRank [30]	93.96	-2.73	8.41×	4.26×
VGG-19	DCP-Adapt [61]	93.99	+0.58	15.58×	2.86×
	SCP [23]	93.84	-0.02	20.88×	3.86×
	NEXP (Ours)	94.00	-0.53	**22.73**×	4.75×

Table 7: Analytical Comparison of Importance-based solutions and Expressiveness on CIFAR-10 using GoogLeNet [45].

Model	Method	top-1 acc Base (%)	Δ (%)	Compression Ratio ↓ #Params	#FLOPs
GoogLeNet	GAL-0.5 [32]	95.05	-0.49	1.97×	1.62×
	NEXP (Ours)	94.97	-0.43	**3.77**×	2.12×
	Hrank [30]	95.05	-0.52	2.25×	2.20×
	ABC [31]	95.05	-0.21	2.51×	2.99×
	NEXP (Ours)	94.97	-1.07	**7.02**×	3.01×
	Hrank [30]	95.05	-0.98	3.31×	3.38×

Table 8: Analytical Comparison of Importance-based solutions and Expressiveness on CIFAR-10 using DenseNet-40 [21].

Model	Method	top-1 acc Base (%)	Δ (%)	Compression Ratio ↓ #Params	#FLOPs
DenseNet-40	GAL-0.5 [32]	95.05	-0.49	1.97×	1.62×
	Hrank [30]	95.05	-0.52	2.25×	2.20×
	NEXP (Ours)	94.64	-0.89	**2.72**×	2.25×
	NEXP (Ours)	94.64	-0.84	**3.12**×	2.51×
	ABC [31]	95.05	-0.21	2.51×	2.99×
	Hrank [30]	95.05	-0.98	3.31×	3.38×

Table 9: Performance Outcomes for MobileNet-v2 on the CIFAR-10 Dataset.

Method	Base (%)	Δ Acc (%)	#Params ↓	#FLOPs ↓
DCP [61]	94.47	+0.22	1.31×	1.36×
NEXP (Ours)	94.32	+0.13	2.25×	2.11×

YOLOv8. Figure 6 compares Neural Expressiveness (NEXP) with Layer-Adaptive Magnitude-Based Pruning (LAMP) [26], Network Slimming (SLIM) [35], Wang et al.'s DepGraph [11], and Random Pruning for Object Detection on the COCO dataset, as discussed in 4.1.

Motivation. YOLOv8 [22] is the current state-of-the-art for Object Detection and Image Segmentation, and has already been widely adopted by many for a variety of real-time applications, e.g. Traffic Safety [1], Medical Imaging [39], Rip Currents Detection [10], and more. Such applications could majorly benefit from model compression optimizations, achieving higher throughput ratios that translate to increased resolution (FPS), and enabling deployment on hardware with strict resource constraints.

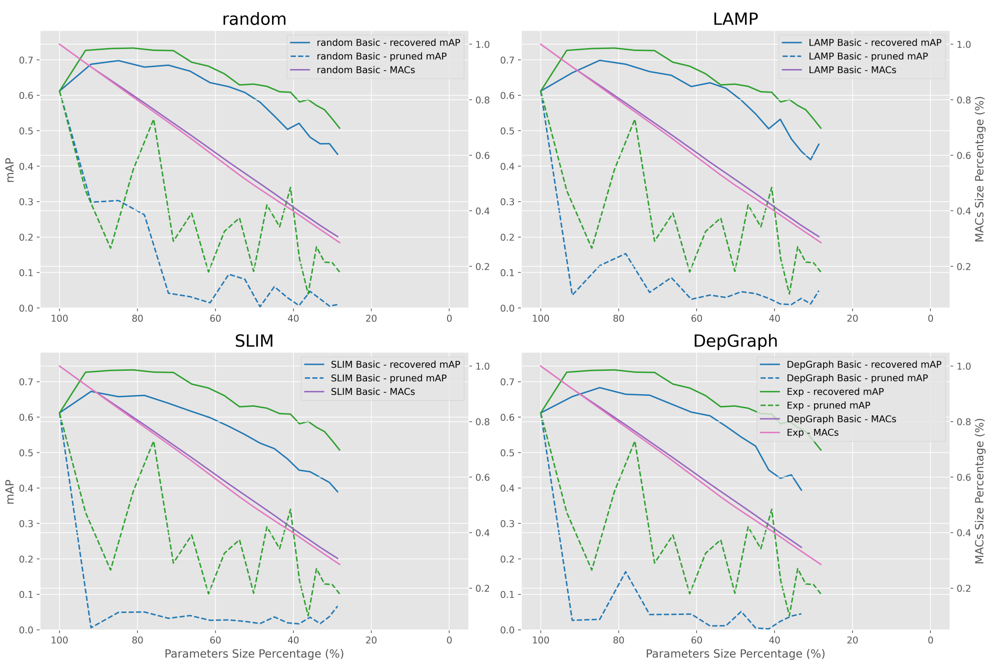

Figure 6: **Pruning YOLOv8m trained on COCO for Object Detection.**

NeurIPS Paper Checklist

1. **Claims**

   Question: Do the main claims made in the abstract and introduction accurately reflect the paper's contributions and scope?

   Answer: [Yes]

   Justification: The main contributions have been reflected and discussed across the whole paper.

   Guidelines:

   - The answer NA means that the abstract and introduction do not include the claims made in the paper.
   - The abstract and/or introduction should clearly state the claims made, including the contributions made in the paper and important assumptions and limitations. A No or NA answer to this question will not be perceived well by the reviewers.
   - The claims made should match theoretical and experimental results, and reflect how much the results can be expected to generalize to other settings.
   - It is fine to include aspirational goals as motivation as long as it is clear that these goals are not attained by the paper.

2. **Limitations**

   Question: Does the paper discuss the limitations of the work performed by the authors?

   Answer: [Yes]

   Justification: While our work does not implicitly provide a Discussion section, we have incorporated any discussions on the limitations and the intricacies of the provided solution at its section separately.

   Guidelines:

   - The answer NA means that the paper has no limitation while the answer No means that the paper has limitations, but those are not discussed in the paper.
   - The authors are encouraged to create a separate "Limitations" section in their paper.
   - The paper should point out any strong assumptions and how robust the results are to violations of these assumptions (e.g., independence assumptions, noiseless settings, model well-specification, asymptotic approximations only holding locally). The authors should reflect on how these assumptions might be violated in practice and what the implications would be.
   - The authors should reflect on the scope of the claims made, e.g., if the approach was only tested on a few datasets or with a few runs. In general, empirical results often depend on implicit assumptions, which should be articulated.
   - The authors should reflect on the factors that influence the performance of the approach. For example, a facial recognition algorithm may perform poorly when image resolution is low or images are taken in low lighting. Or a speech-to-text system might not be used reliably to provide closed captions for online lectures because it fails to handle technical jargon.
   - The authors should discuss the computational efficiency of the proposed algorithms and how they scale with dataset size.
   - If applicable, the authors should discuss possible limitations of their approach to address problems of privacy and fairness.
   - While the authors might fear that complete honesty about limitations might be used by reviewers as grounds for rejection, a worse outcome might be that reviewers discover limitations that aren't acknowledged in the paper. The authors should use their best judgment and recognize that individual actions in favor of transparency play an important role in developing norms that preserve the integrity of the community. Reviewers will be specifically instructed to not penalize honesty concerning limitations.

3. **Theory Assumptions and Proofs**

   Question: For each theoretical result, does the paper provide the full set of assumptions and a complete (and correct) proof?

Answer: [Yes]

Justification: To the best of our knowledge, all the provided set of assumptions presented in Section 3 are complete.

Guidelines:

- The answer NA means that the paper does not include theoretical results.
- All the theorems, formulas, and proofs in the paper should be numbered and cross-referenced.
- All assumptions should be clearly stated or referenced in the statement of any theorems.
- The proofs can either appear in the main paper or the supplemental material, but if they appear in the supplemental material, the authors are encouraged to provide a short proof sketch to provide intuition.
- Inversely, any informal proof provided in the core of the paper should be complemented by formal proofs provided in appendix or supplemental material.
- Theorems and Lemmas that the proof relies upon should be properly referenced.

4. **Experimental Result Reproducibility**

Question: Does the paper fully disclose all the information needed to reproduce the main experimental results of the paper to the extent that it affects the main claims and/or conclusions of the paper (regardless of whether the code and data are provided or not)?

Answer: [Yes]

Justification: The paper specifies in great detail all the information necessary to understand the results, while also any subjectivity imposed by the experimental settings in regards to our claims and conclusions has been discussed. Detailed analysis of both the mathematical, technical and experimental intricacies have been included in our work.

Guidelines:

- The answer NA means that the paper does not include experiments.
- If the paper includes experiments, a No answer to this question will not be perceived well by the reviewers: Making the paper reproducible is important, regardless of whether the code and data are provided or not.
- If the contribution is a dataset and/or model, the authors should describe the steps taken to make their results reproducible or verifiable.
- Depending on the contribution, reproducibility can be accomplished in various ways. For example, if the contribution is a novel architecture, describing the architecture fully might suffice, or if the contribution is a specific model and empirical evaluation, it may be necessary to either make it possible for others to replicate the model with the same dataset, or provide access to the model. In general. releasing code and data is often one good way to accomplish this, but reproducibility can also be provided via detailed instructions for how to replicate the results, access to a hosted model (e.g., in the case of a large language model), releasing of a model checkpoint, or other means that are appropriate to the research performed.
- While NeurIPS does not require releasing code, the conference does require all submissions to provide some reasonable avenue for reproducibility, which may depend on the nature of the contribution. For example
  (a) If the contribution is primarily a new algorithm, the paper should make it clear how to reproduce that algorithm.
  (b) If the contribution is primarily a new model architecture, the paper should describe the architecture clearly and fully.
  (c) If the contribution is a new model (e.g., a large language model), then there should either be a way to access this model for reproducing the results or a way to reproduce the model (e.g., with an open-source dataset or instructions for how to construct the dataset).
  (d) We recognize that reproducibility may be tricky in some cases, in which case authors are welcome to describe the particular way they provide for reproducibility. In the case of closed-source models, it may be that access to the model is limited in some way (e.g., to registered users), but it should be possible for other researchers to have some path to reproducing or verifying the results.

5. **Open access to data and code**

Question: Does the paper provide open access to the data and code, with sufficient instructions to faithfully reproduce the main experimental results, as described in supplemental material?

Answer: [No]

Justification: We plan to release the full code of the implementation and experiments upon acceptance.

Guidelines:

- The answer NA means that paper does not include experiments requiring code.
- Please see the NeurIPS code and data submission guidelines (`https://nips.cc/public/guides/CodeSubmissionPolicy`) for more details.
- While we encourage the release of code and data, we understand that this might not be possible, so "No" is an acceptable answer. Papers cannot be rejected simply for not including code, unless this is central to the contribution (e.g., for a new open-source benchmark).
- The instructions should contain the exact command and environment needed to run to reproduce the results. See the NeurIPS code and data submission guidelines (`https://nips.cc/public/guides/CodeSubmissionPolicy`) for more details.
- The authors should provide instructions on data access and preparation, including how to access the raw data, preprocessed data, intermediate data, and generated data, etc.
- The authors should provide scripts to reproduce all experimental results for the new proposed method and baselines. If only a subset of experiments are reproducible, they should state which ones are omitted from the script and why.
- At submission time, to preserve anonymity, the authors should release anonymized versions (if applicable).
- Providing as much information as possible in supplemental material (appended to the paper) is recommended, but including URLs to data and code is permitted.

6. **Experimental Setting/Details**

Question: Does the paper specify all the training and test details (e.g., data splits, hyperparameters, how they were chosen, type of optimizer, etc.) necessary to understand the results?

Answer: [Yes]

Justification: The paper specifies all the training and test details necessary to understand the results. Each experiment is accompanied by a discussion of its experimental details and a reference to its experimental settings (Section 4). Additionally, an overview of the experiment settings can be found in Appendix C, and an in-depth analysis of the pruning procedure, including its implementation choices, is described in Appendix B.

Guidelines:

- The answer NA means that the paper does not include experiments.
- The experimental setting should be presented in the core of the paper to a level of detail that is necessary to appreciate the results and make sense of them.
- The full details can be provided either with the code, in appendix, or as supplemental material.

7. **Experiment Statistical Significance**

Question: Does the paper report error bars suitably and correctly defined or other appropriate information about the statistical significance of the experiments?

Answer: [No]

Justification: While we do not explicitly address the statistical significance of each experiment (in a quantitative manner), we do discuss in great detail any assumptions or statistical implications of our experiments (in a qualitative manner).

Guidelines:

- The answer NA means that the paper does not include experiments.

- The authors should answer "Yes" if the results are accompanied by error bars, confidence intervals, or statistical significance tests, at least for the experiments that support the main claims of the paper.
- The factors of variability that the error bars are capturing should be clearly stated (for example, train/test split, initialization, random drawing of some parameter, or overall run with given experimental conditions).
- The method for calculating the error bars should be explained (closed form formula, call to a library function, bootstrap, etc.)
- The assumptions made should be given (e.g., Normally distributed errors).
- It should be clear whether the error bar is the standard deviation or the standard error of the mean.
- It is OK to report 1-sigma error bars, but one should state it. The authors should preferably report a 2-sigma error bar than state that they have a 96% CI, if the hypothesis of Normality of errors is not verified.
- For asymmetric distributions, the authors should be careful not to show in tables or figures symmetric error bars that would yield results that are out of range (e.g. negative error rates).
- If error bars are reported in tables or plots, The authors should explain in the text how they were calculated and reference the corresponding figures or tables in the text.

8. **Experiments Compute Resources**

   Question: For each experiment, does the paper provide sufficient information on the computer resources (type of compute workers, memory, time of execution) needed to reproduce the experiments?

   Answer: [Yes]

   Justification: While we do not provide the exact times of executions and memory requirements for each experiment, we do provide an in-depth analysis of all the parameters and experimental specifications, along side with the overview of the configurations that were used for this work Appendix C and Section 4.

   Guidelines:

   - The answer NA means that the paper does not include experiments.
   - The paper should indicate the type of compute workers CPU or GPU, internal cluster, or cloud provider, including relevant memory and storage.
   - The paper should provide the amount of compute required for each of the individual experimental runs as well as estimate the total compute.
   - The paper should disclose whether the full research project required more compute than the experiments reported in the paper (e.g., preliminary or failed experiments that didn't make it into the paper).

9. **Code Of Ethics**

   Question: Does the research conducted in the paper conform, in every respect, with the NeurIPS Code of Ethics `https://neurips.cc/public/EthicsGuidelines`?

   Answer: [Yes]

   Justification: We have thoroughly reviewed the research conducted in the paper and fully agree that it conforms to the NeurIPS Code of Ethics.

   Guidelines:

   - The answer NA means that the authors have not reviewed the NeurIPS Code of Ethics.
   - If the authors answer No, they should explain the special circumstances that require a deviation from the Code of Ethics.
   - The authors should make sure to preserve anonymity (e.g., if there is a special consideration due to laws or regulations in their jurisdiction).

10. **Broader Impacts**

    Question: Does the paper discuss both potential positive societal impacts and negative societal impacts of the work performed?

Answer: [NA]

Justification: While our work does not directly discuss societal impacts, we do reference the eco-friendly implications of efficient models in the Introduction section 1. Additionally, we highlight the potential indirect societal benefits that can arise from optimizing models, such as in the case of YOLOv8 D.2. .

Guidelines:

- The answer NA means that there is no societal impact of the work performed.
- If the authors answer NA or No, they should explain why their work has no societal impact or why the paper does not address societal impact.
- Examples of negative societal impacts include potential malicious or unintended uses (e.g., disinformation, generating fake profiles, surveillance), fairness considerations (e.g., deployment of technologies that could make decisions that unfairly impact specific groups), privacy considerations, and security considerations.
- The conference expects that many papers will be foundational research and not tied to particular applications, let alone deployments. However, if there is a direct path to any negative applications, the authors should point it out. For example, it is legitimate to point out that an improvement in the quality of generative models could be used to generate deepfakes for disinformation. On the other hand, it is not needed to point out that a generic algorithm for optimizing neural networks could enable people to train models that generate Deepfakes faster.
- The authors should consider possible harms that could arise when the technology is being used as intended and functioning correctly, harms that could arise when the technology is being used as intended but gives incorrect results, and harms following from (intentional or unintentional) misuse of the technology.
- If there are negative societal impacts, the authors could also discuss possible mitigation strategies (e.g., gated release of models, providing defenses in addition to attacks, mechanisms for monitoring misuse, mechanisms to monitor how a system learns from feedback over time, improving the efficiency and accessibility of ML).

11. **Safeguards**

    Question: Does the paper describe safeguards that have been put in place for responsible release of data or models that have a high risk for misuse (e.g., pretrained language models, image generators, or scraped datasets)?

    Answer: [NA]

    Justification: Our work emphasizes on efficiently compressing Neural Networks and does not target any specific use-case scenario, rather it addresses the greater challenge of Vision as whole.

    Guidelines:

    - The answer NA means that the paper poses no such risks.
    - Released models that have a high risk for misuse or dual-use should be released with necessary safeguards to allow for controlled use of the model, for example by requiring that users adhere to usage guidelines or restrictions to access the model or implementing safety filters.
    - Datasets that have been scraped from the Internet could pose safety risks. The authors should describe how they avoided releasing unsafe images.
    - We recognize that providing effective safeguards is challenging, and many papers do not require this, but we encourage authors to take this into account and make a best faith effort.

12. **Licenses for existing assets**

    Question: Are the creators or original owners of assets (e.g., code, data, models), used in the paper, properly credited and are the license and terms of use explicitly mentioned and properly respected?

    Answer: [Yes]

Justification: All the creators and original owners of the assets that were utilized for this work were properly credited through-out all parts of the paper, while also a detailed report of them can be found in Appendix C.

Guidelines:

- The answer NA means that the paper does not use existing assets.
- The authors should cite the original paper that produced the code package or dataset.
- The authors should state which version of the asset is used and, if possible, include a URL.
- The name of the license (e.g., CC-BY 4.0) should be included for each asset.
- For scraped data from a particular source (e.g., website), the copyright and terms of service of that source should be provided.
- If assets are released, the license, copyright information, and terms of use in the package should be provided. For popular datasets, `paperswithcode.com/datasets` has curated licenses for some datasets. Their licensing guide can help determine the license of a dataset.
- For existing datasets that are re-packaged, both the original license and the license of the derived asset (if it has changed) should be provided.
- If this information is not available online, the authors are encouraged to reach out to the asset's creators.

13. **New Assets**

Question: Are new assets introduced in the paper well documented and is the documentation provided alongside the assets?

Answer: [NA]

Justification: The paper does not release new assets besides the conceptualization and both then technical and theoretical formulation of Neural Expressiveness. However, we plan to release the full code of the implementation and experiments upon acceptance.

Guidelines:

- The answer NA means that the paper does not release new assets.
- Researchers should communicate the details of the dataset/code/model as part of their submissions via structured templates. This includes details about training, license, limitations, etc.
- The paper should discuss whether and how consent was obtained from people whose asset is used.
- At submission time, remember to anonymize your assets (if applicable). You can either create an anonymized URL or include an anonymized zip file.

14. **Crowdsourcing and Research with Human Subjects**

Question: For crowdsourcing experiments and research with human subjects, does the paper include the full text of instructions given to participants and screenshots, if applicable, as well as details about compensation (if any)?

Answer: [NA]

Justification: Our paper does not involve crowdsourcing nor research with human subjects.

Guidelines:

- The answer NA means that the paper does not involve crowdsourcing nor research with human subjects.
- Including this information in the supplemental material is fine, but if the main contribution of the paper involves human subjects, then as much detail as possible should be included in the main paper.
- According to the NeurIPS Code of Ethics, workers involved in data collection, curation, or other labor should be paid at least the minimum wage in the country of the data collector.

15. **Institutional Review Board (IRB) Approvals or Equivalent for Research with Human Subjects**

Question: Does the paper describe potential risks incurred by study participants, whether such risks were disclosed to the subjects, and whether Institutional Review Board (IRB) approvals (or an equivalent approval/review based on the requirements of your country or institution) were obtained?

Answer: [NA]

Justification: Our paper does not involve crowdsourcing nor research with human subjects.

Guidelines:

- The answer NA means that the paper does not involve crowdsourcing nor research with human subjects.
- Depending on the country in which research is conducted, IRB approval (or equivalent) may be required for any human subjects research. If you obtained IRB approval, you should clearly state this in the paper.
- We recognize that the procedures for this may vary significantly between institutions and locations, and we expect authors to adhere to the NeurIPS Code of Ethics and the guidelines for their institution.
- For initial submissions, do not include any information that would break anonymity (if applicable), such as the institution conducting the review.